Molecular pathway for thymoquinone-induced cell-cycle arrest and apoptosis in neoplastic keratinocytes

Hala U. Gali-Muhtasib[a], Wassim G. Abou Kheir[a], Lynn A. Kheir[a], Nadine Darwiche[a] and Peter A. Crooks[b]

Thymoquinone (TQ), the most abundant constituent in black seed, was shown to possess potent chemopreventive activities against DMBA-initiated TPA-promoted skin tumors in mice. Despite the potential interest in TQ as a skin antineoplastic agent, its mechanism of action has not been examined yet. Using primary mouse keratinocytes, papilloma (SP-1) and spindle (I7) carcinoma cells, we studied the cellular and molecular events involved in TQ's antineoplastic activity. We show that non-cytotoxic concentrations of TQ reduce the proliferation of neoplastic keratinocytes by 50%. The sensitivity of cells to TQ treatment appears to be stage dependent such that papilloma cells are twice as sensitive to the growth inhibitory effects of TQ as the spindle cancer cells. TQ treatment of SP-1 cells induced G_0/G_1 cell-cycle arrest, which correlated with sharp increases in the expression of the cyclin-dependent kinase inhibitor p16 and a decrease in cyclin D_1 protein expression. TQ-induced growth inhibition in I7 cells by inducing G_2/M cell-cycle arrest, which was associated with an increase in the expression of the tumor suppressor protein p53 and a decrease in cyclin B_1 protein. At longer times of incubation, TQ induced apoptosis in both cell lines by remarkably increasing the ratio of Bax/Bcl-2 protein expression and decreasing Bcl-x_L protein. The apoptotic effects of TQ were more pronounced in SP-1 than in I7 cells. Collectively, these findings support a potential role for TQ as a chemopreventive agent, particularly at the early stages of skin tumorigenesis. *Anti-Cancer Drugs* 15:389–399

Anti-Cancer Drugs 2004, **15**:389–399

Keywords: apoptosis, black seed, cell-cycle arrest, chemoprevention, keratinocyte, neoplasia, skin, thymoquinone

[a]Department of Biology, American University of Beirut, Beirut, Lebanon and [b]College of Pharmacy, University of Kentucky, Lexington, KY, USA.

Sponsorship: This work was supported by the University Research Board of the American University of Beirut and the Lebanese National Council for Scientific Research.

Correspondence to H. U. Gali-Muhtasib, Department of Biology, American University of Beirut, Beirut, Lebanon.
Tel: +961 3973820; fax: +961 1744461;
e-mail: amro@aub.edu.lb

Received 8 November 2003 **Accepted** 10 January 2004

Introduction

Skin cancer is the most common form of cancer in the US, more common than all other cancers combined [1]. The two most common types of human skin cancers are basal and squamous cell carcinomas, which are grouped together as non-melanoma skin cancer (NMSC). The incidence of NMSCs was estimated at 1.3 million cases for the year 2000 and is on the rise. Continued increases in NMSC incidence rates are expected as the population ages and larger amounts of ultraviolet radiation reach the Earth's surface due to depletion of the ozone layer [2]. Therefore, the development of new drugs with potential to provide more selective treatments is a topic of intense investigation.

Herbal therapies are commonly used for the prevention and treatment of cancer despite little understanding about their molecular and cellular basis of action. Black seed (*Nigella sativa*) is an annual herb of the Ranunculaceae family which grows in countries bordering the Mediterranean Sea, Pakistan and India. This plant has been used in traditional medicine by Asian and Far Eastern countries as a spice and food preservative, and a protective and health remedy in traditional folk medicine for the treatment of numerous disorders [3]. The seeds of this plant are very rich and diverse in chemical composition. Among the chemical components of black seed, thymoquinone (TQ) is the most abundant active principle and the most extensively investigated. The preparations from this plant have been demonstrated to have significant antineoplastic activity against various tumor cells *in vitro* [4,5]. TQ's antineoplastic activities were demonstrated against human pancreatic adenocarcinoma, uterine sarcoma, Ehrlich ascites carcinoma and Dalton's ascites lymphoma, while exerting minimal cytotoxicity to normal lymphocytes [6]. Several studies have shown that TQ retards the carcinogenic process in animals. TQ was shown to inhibit tumor formation in DMBA-initiated TPA-promoted mouse skin [4]. A dose of 100 mg/kg body weight of *N. sativa* extract delayed the onset of papilloma formation and reduced the mean number of papillomas per mouse [4–6]. The protective actions of TQ have been suggested to be through its antioxidant and anti-inflammatory activities [7]. Despite

0959-4973 © 2004 Lippincott Williams & Wilkins DOI: 10.1097/01.cad.0000125054.43188.56

TQ's interesting potential as an antineoplastic agent, the cellular and molecular events involved in its action have not been examined yet.

The tumor suppressor p53 is the most commonly mutated gene in human cancers [8]. Cells can respond to the activation of the tumor suppressor protein p53 by undergoing cell-cycle arrest or apoptosis [9]. Active p53 is able to stimulate the transcription of a variety of genes including $p21^{WAF1}$, which is a universal inhibitor of the cyclin-dependent kinases (CDK) [10,11]. $p21^{WAF}$ overexpression is thought to be a major mediator of p53-dependent G_1 arrest, is required to arrest cells at the G_1 and G_2 checkpoints of the cell cycle after DNA damage [12,13], and is associated with a reduction of cyclin B_1 expression [14]. In contrast to $p21^{WAF1}$, the overexpression of Bcl-2 protein has been shown to inhibit p53-mediated apoptosis as well as p53-mediated transcriptional activation [15]. In addition, $p16^{INK4a}$, a recognized tumor suppressor, induces G_1 cell-cycle arrest by binding to CDK4, and inhibiting its ability to interact with cyclin D and stimulate passage through the G_1 phase of the cell cycle. In this study we show that treatment of neoplastic keratinocytes with TQ remarkably inhibits their proliferation at concentrations non-cytotoxic to primary mouse keratinocytes. Interestingly, the SP-1 papilloma cell line was more sensitive to the growth inhibitory effects of TQ, suggesting that the sensitivity to TQ treatment is dependent on the stage of tumorigenesis. Cell growth inhibition achieved by TQ treatment was correlated with G_1 and G_2 phase arrest of the cell cycle followed by apoptosis. These findings support a potential role for TQ as a skin antineoplastic agent, especially at the early tumorigenesis stages.

Materials and methods

Media and chemicals

Eagle's minimum essential Eagle medium (EMEM) was obtained from Biowhittaker (Walkersville, MD). Fetal bovine serum (FBS), dialyzed FBS, L-glutamine, penicillin/streptomycin, 10 × trypsin–EDTA, 0.25 × trypsin–EDTA, Dulbecco's phosphate-buffered saline (PBS) and dispase were obtained from Gibco/BRL Life Technologies Minneapolis, MN). Propidium iodide and Prolong Antifade were purchased from Molecular Probes (Eugene, OR). Trypan blue and RNase A were obtained from Sigma (St Louis, MO). The DC Protein Assay was obtained from Bio-Rad (Hercules, CA). The luminescent kit as well as the p21((C-19)-G) antibody, actin (I-19) antibody, cyclin B_1 (H-433), anti-mouse IgG–horseradish peroxidase (HRP), anti-rabbit IgG–HRP and anti-goat IgG–HRP secondary antibodies were purchased from Santa Cruz Biotechnology (Santa Cruz, CA). The Bax, Bcl-x_L (2H12), Bcl-2 (N-19), p53 (DO12), p16 (M-156) and cyclin D (M-20) antibodies were purchased from Biosource (Irvine, CA). A purified preparation of TQ (> 99% pure) was kindly provided by Dr Peter Crooks (Lexington, KY).

Cell culture and treatment

SP-1 and I7 cells were kindly provided by Dr S. H. Yuspa (NIH, Bethesda, MD). Mouse papilloma SP-1 cells and primary mouse keratinocytes (PMK) were cultured in EMEM supplemented with 8% dialyzed FBS, 2 mM L-glutamine, 100 U/ml penicillin and 100 μg/ml streptomycin. I7 cells were cultured in EMEM medium supplemented with 8% FBS. Cells were grown in a humidified incubator (95% air/5% CO_2) and media was replenished every 2 days. PMK were prepared by sacrificing 1-day-old BALB/c mice on ice for 45 min. Mouse skin was washed twice with betadine and distilled water, and the epidermis was separated from the dermis by an overnight incubation at 4°C in serum-free medium containing 0.25% dispase. Following trypsinization (0.25 × trypsin–EDTA, 37°C for 15 min), the cell suspension was filtered using cell strainers and cells were plated in their respective medium at a density of two-mouse equivalents per 100-mm tissue culture dish. For all experiments, cells were treated with TQ at 40–50% confluency with defined concentrations of TQ dissolved in methanol. The methanol concentration in treated and control wells did not exceed 0.1%/well.

Cell proliferation and viability assays

Cell proliferation and cytotoxicity were determined using the CellTiter 96 Non-Radioactive Cell Proliferation Assay and the CytoTox 96 Non-Radioactive Cytotoxicity Assay (both kits from Promega, Madison, WI) according to the manufacturer's suggestions. The proliferation assay is an MTT-based method which measures the ability of metabolically active cells to convert tetrazolium salt into a cleavage product and its absorbance is recorded at 570 nm. The CytoTox 96 assay quantitatively measures the lactate dehydrogenase (LDH), a stable cytosolic enzyme that is released upon cell lysis [16]. Released LDH in culture supernatants is measured with a coupled enzymatic assay which results in the conversion of a tetrazolium salt into a red formazan product, the absorbance of which is recorded at 490 nm.

Flow cytometric analysis of DNA content

Cells were seeded in 100-mm dishes at a density of 7.5×10^5 cells/well. They were incubated and allowed to grow to 40–50% confluence after which they were treated with concentrations of TQ and incubated for further a 24 or 48 h. They were then harvested by trypsin release, washed twice with PBS, permeabilized with 70% ethanol, treated with 1% RNase and finally stained with propidium iodide (100 μg/ml final concentration). Distribution of cell-cycle phases with different DNA contents was determined using a FACScan flow cytometer (Becton Dickinson, San Jose, CA). Cells that were less intensely stained than G_1 cells (sub-G_1 cells) in

flow cytometric histograms were considered apoptotic cells. Analysis of cell-cycle distribution and the percentage of cells in the G_1, S and G_2/M phases of the cell cycle were determined using CellQuest.

Apoptosis: TUNEL assay

Apoptosis was scored either by assessing the fraction of cells with a sub-G_0/G_1 DNA content by flow cytometry (see above) or by estimating the extent of DNA fragmentation by the TUNEL assay. Briefly, cells were plated on autoclaved glass coverslips in six-well culture plates and treated with TQ or PFT-α as described earlier. The medium was then aspirated and cells were washed twice with warm PBS. Cellular DNA was stained with the *In situ* Cell Death Detection kit (Roche Diagnostics, Mannheim, Germany) and the assay performed according to the recommendations of the manufacturer (Boehringer, Mannheim, Germany). A positive control of DNase treatment was included in the assay. Cytospin preparations were fixed and labeled, and four independent × 100 fields containing a minimum of 300 cells on each of three replicate slides were evaluated for nuclear labeling by fluorescence microscopy (Axiovert 200; Zeiss, Intermedic, Gottingen, Germany) for each treatment. Nuclear chromatin condensation was observed under fluorescence microscopy (LSM 410; Zeiss).

RNase protection assay

The RiboQuant Multiprobe protection assay system (PharMingen, San Diego, CA) is a highly sensitive and specific method for simultaneous detection and quantification of multiple mRNA species. Mouse apoptosis template probe sets are available to detect levels of Bcl-2, Bax, Bcl-x, Bcl-w, L32 and GAPDH. After isolating RNA from the tissues of interest, the antisense RNA probe was hybridized in excess to target RNA in solution. Free probe and non-hybridized single-stranded RNA were digested with RNases. ^{32}P-labeled antisense RNA was transcribed using T7 RNA polymerase (PharMingen) and [α-^{32}P]UTP (Amersham Life Science, Piscataway, NJ). The reaction was terminated after 1 h at room temperature by the addition of DNase. Total RNA was extracted from tissue using TRIzol (Gibco Life Technologies, Carlsbad, CA). Total RNA (15–20 μg) was hybridized with the ^{32}P-labeled RNA probes that were transcribed from the customized multiprobes (DNA templates) at 56°C overnight, followed by digestion with RNase A for 45 min at 30°C which is then terminated by addition of proteinase K. Single-stranded and unhybridized excess mRNA was digested by RNase A. The protected double-stranded RNA pellets were dried and resuspended in 5 μl of 1 × loading buffer (PharMingen) and electrophoretically resolved on 5% polyacrylamide–8 M urea gel. The polyacrylamide–urea gel was dried on blotting paper for 1 h at 80°C. The labeled probes then were quantified by autoradiography. Yeast tRNA was used as a negative control.

Radioanalytic imaging

For comparative analysis, we quantified mRNA levels as a percentage of the ribosomal protein L32 mRNA level. Radioactivity of each band in the sample was quantified, standardized and compared with the level of L32 detected in that sample. Radioactivity of each template was quantified directly from the gel by a radioanalytic imaging system (UVP Digidoc-it; UVP, Upland, CA). Net counts were obtained from each template (band) including L32 and the results were expressed as percentage of control cells for each group after normalization to L32.

Protein extraction and Western blot analysis

Cellular proteins were extracted from cells in buffer containing 50 mM Tris–HCl, pH 7.5, 150 mM NaCl, 1% Nonidet P-40, 0.5% sodium deoxycholate, 4% protease inhibitors and 1% phosphatase inhibitors. The cell lysate was rotated at 4°C for 30 min, centrifuged at 10 000 r.p.m. for 10 min and the precipitates discarded. Protein concentrations were determined by the DC Bio-Rad protein assay kit using bovine serum albumin as a standard. Cellular protein (25 μg) was loaded onto 10% SDS–polyacrylamide gels. The proteins were then transferred to a PVDF membrane (NEN Life Sciences Products, Boston, MA) which was then incubated with primary antibody. HRP-conjugated goat anti-rabbit or goat anti-mouse IgGs were used as secondary antibodies as appropriate. The immunoreactive bands were visualized on X-ray film (Hyperfilm ECL) using a chemiluminescent substrate (Amersham). The β-actin antibody (HHF35) was used to ensure equal protein loading.

Results

Effects of TQ on growth of primary and neoplastic keratinocytes

We determined whether TQ is toxic to PMK cells following treatment with graded concentrations of TQ (20–100 μM) for 12 h (Fig. 1). Cell growth and survival was not affected by treatment of PMK with concentrations up to 80 μM TQ. Higher concentrations of 100 μM TQ reduced the viability of PMK by 60% at 12 h compared to control cells. Next, we determined whether TQ affects the growth of neoplastic keratinocytes at progressive stages of tumorigenesis. We used a murine *in vitro* model of skin carcinogenesis which consists of papilloma and spindle cell lines. We chose a well-characterized SP-1 cell line that produces benign papillomas when grafted onto the dorsum of immune-deficient mice [17]. We also chose an advanced I7 spindle cell line derived from keratinocytes transduced with v-*ras*^{Ha} and v-*fos* oncogenes grafted to nude mice [18]. The effects of TQ on neoplastic keratinocytes were studied by determining whether TQ at various concentrations is: (i) cytotoxic to SP-1 and I7 cells for up to 1 day post-TQ treatment, (ii) suppresses the proliferation of neoplastic cells for up to 2 days post-treatment, and (iii) causes

Fig. 1

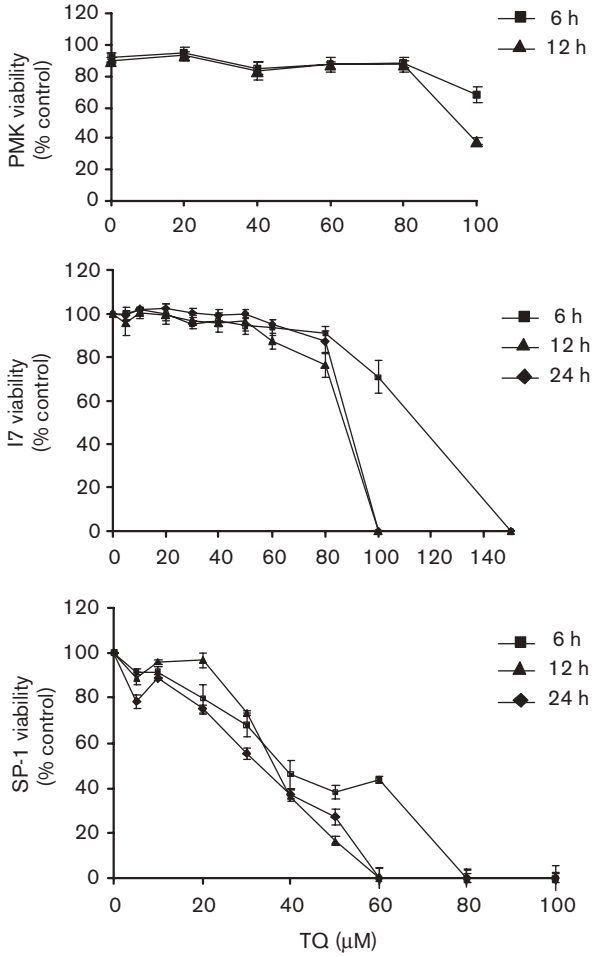

TQ treatment causes a dose- and time-dependent decrease in the viability of SP-1 and I7 cells, but not PMKs. Cells were plated in 96-well plates at a density of 0.75×10^5 cells/ml. At 40–60% confluency, cells were treated with less than 0.1% methanol or TQ for up to 24 h. The plots indicate viability of control and TQ-treated cells over a period of 24 h. Viability was assessed as described in Materials and methods. Results are expressed as percentage of methanol-treated cells for each group. The values depict an average (±SD) of quadruplicate measurements. Results are representative of at least two independent experiments.

Fig. 2

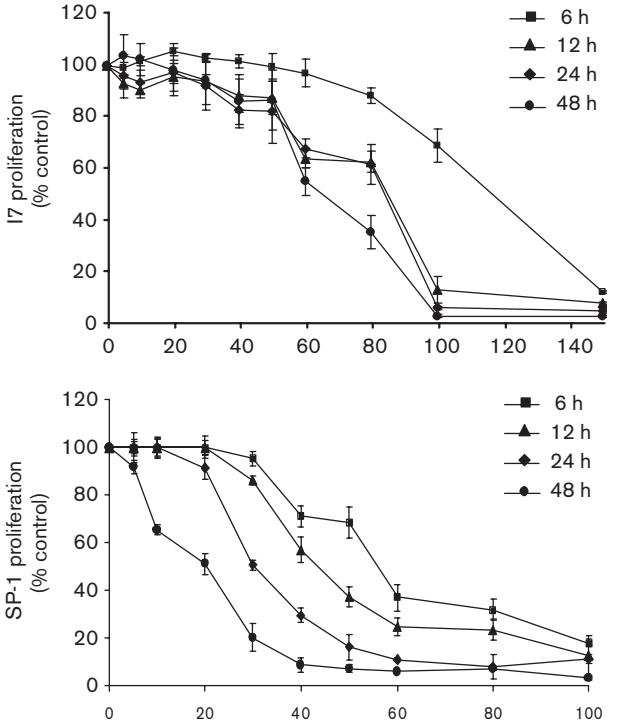

TQ treatment causes a dose- and time-dependent growth suppression in I7 and SP-1 cells. Cells were plated in 96-well plates at a density of 0.75×10^5 cells/ml. At 40–60% confluency, cells were treated with less than 0.1% methanol or TQ for up to 24 h. The graphs indicate viability of control and TQ-treated cells over a period of 48 h. Growth was assessed as described in Materials and methods. Results are expressed as percentage of methanol-treated cells for each group. The values depict an average (±SD) of quadruplicate measurements. Results are representative of at least two independent experiments.

visible morphological changes in SP-1 and I7 cells. Towards this end, cells were treated with TQ and cellular toxicity was determined using the CytoTox 96 assay. We noted that the more aggressive I7 spindle cells were less sensitive to the toxic effects of TQ (Fig. 1). No signs of toxicity to I7 cells were observed at doses of up to 80 μM TQ, while concentrations of 30 μM reduced SP-1 cell viability by almost 40% (Fig. 1). Similarly, I7 cells were more resistant than SP-1 cells to the growth suppressive effects of TQ (Fig. 2). TQ remarkably inhibited the proliferation of SP-1 papilloma cells in a dose- and time-dependent manner (Fig. 2) with IC_{50} (50% inhibitory concentrations) values of 55, 45, 30 and 20 after 6, 12, 24 and 48 h, respectively. The 50% inhibitory concentrations of TQ were used to determine the time-course effects of TQ on cell morphology. These concentrations were 30 μM for SP-1 cells and 60 μM for I7 cells. Treatment of SP-1 cells with 30 μM TQ induced visible alterations in the cell morphology as early as 4 h post-treatment. A clear loss of basal-like appearance and the impaired ability of SP-1 cells to become confluent were noted (Fig. 3). Treatment of I7 cells with 60 μM of TQ also resulted in significant alterations in cell morphology as early as 8 h post-treatment (Fig. 3). Furthermore, the growth of these cells decreased with time as cells were less confluent than methanol-treated control cells.

Effect of TQ on cell-cycle distribution of neoplastic keratinocytes

To dissect the mechanism for the anti-proliferative effects of TQ, we determined whether the growth inhibitory effects of TQ are associated with specific changes in cell-cycle progression. Neoplastic keratino-

Fig. 3

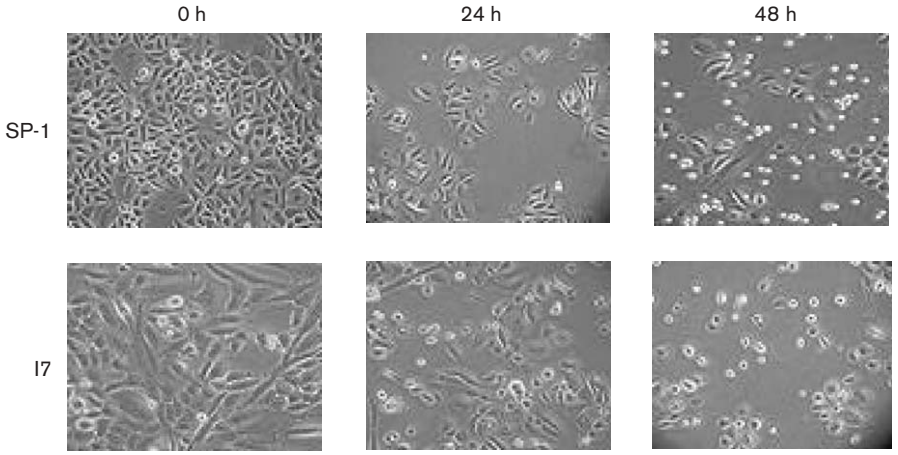

TQ treatment alters the morphology of SP-1 and I7 cells. Cells were plated in 100-mm culture dishes at a density of 2×10^5 cells/ml. At 40–60% confluency, cells were treated with less than 0.1% methanol, 30 μM TQ for SP-1 cells and 60 μM TQ for I7 cells for various time points.

Fig. 4

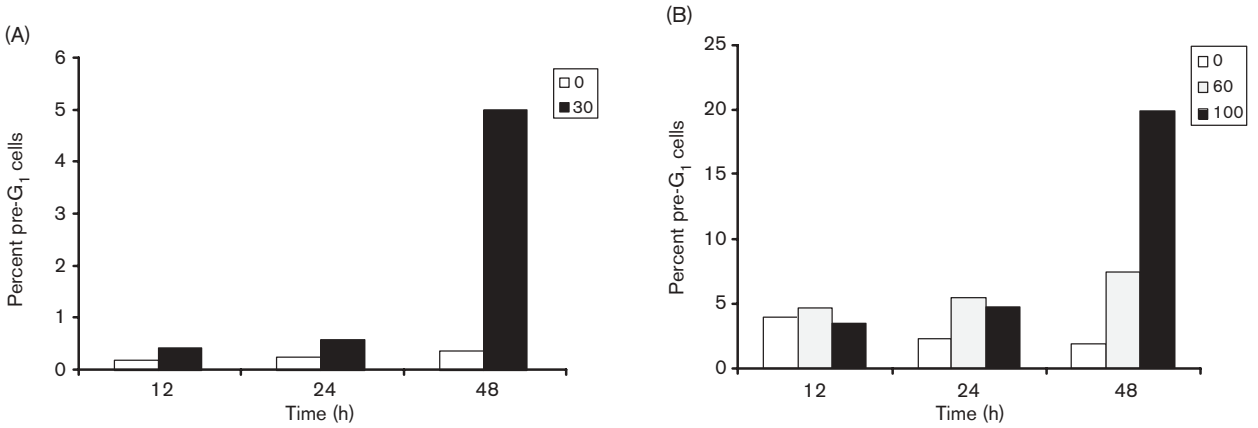

Percentage of pre-G_1 cells after treatment with 30 or 60 μM of TQ in SP-1 (A) and I7 (B) cells, respectively. DNA was stained with propidium iodide and DNA content was then quantified by flow cytometry. The distribution of cells in the pre-G_1 phase of the cell cycle was determined using the CellQuest histogram analysis program. Results are representatives of two independent experiments.

Table 1 Cell-cycle distribution in SP-1 and 17 cells following TQ treatment for 12, 24 and 48 h

SP-1 cells	12 h			24 h			
	C		30 μM	C			30 μM
G_0/G_1	50.2		57.4	50.8			61.3
S	15.6		8.1	14.2			8.2
G_2M	34.0		34.1	34.8			29.9
I7 cells	12 h				24 h			
	C	20 μM	60 μM	100 μM	C	20 μM	60 μM	100 μM
G_0G_1	44.7	48.4	33.3	34.3	44.3	42.4	34.6	34.4
S	17.4	13.2	12.5	14.9	14.8	17.1	8.4	10.4
G_2M	32.3	35.2	45.0	44.2	36.1	36.3	46.1	46.8

SP-1 cells were treated with 30 μM TQ and I7 cells were treated with 20, 60, or 100 μM TQ for 12, 24 and 48 h and stained with propidium iodide. DNA content was then quantified by flow cytometry. The distribution of cells in the various phases of the cell cycle was determined using the CellQuest histogram analysis program. Results are representatives of two independent experiments.

cytes were treated with TQ for 12–48 h and harvested for flow cytometric analysis of DNA content by propidium iodide staining. For SP-1 cells, we used IC_{50} concentrations (30 μM) achieved at 24 h following TQ treatment to investigate whether the inhibition of cell proliferation by TQ was due to cell-cycle arrest and/or apoptosis. For the more resistant I7 cells, a range of TQ concentrations (20, 60 and 100 μM) were investigated. As summarized in Table 1, TQ treatment of SP-1 cells with 30 μM caused an increase, within 12 h, in the number of cells in the G_1 phase of the cell cycle, providing evidence of G_1 arrest. At 24 h post-treatment, the G_1 population increased from 50% in the control to 61% in SP-1 cells treated with TQ with a concomitant decrease in the percentage of S phase cells (Table 1). At longer incubation times of 48 h, the accumulation of a pre-G_1 peak of hypodiploid cells to the left of the G_1 peak was evident (Fig. 4). Upon treatment of I7 cells with 60 μM TQ, a 28% increase in the percentage of cells in G_2/M phase was noted at 24 h post-treatment (Table 1). These results indicate that at short incubation times, TQ is involved in G_1/S-phase arrest in SP-1 cells and G_2/M arrest in I7 cells; however, at long incubation times TQ induces apoptosis in both cell lines (Fig. 4).

To understand and confirm the nature of cell death, we utilized the TUNEL assay method in which FITC-conjugated dUTP was incorporated into the DNA strand

Fig. 5

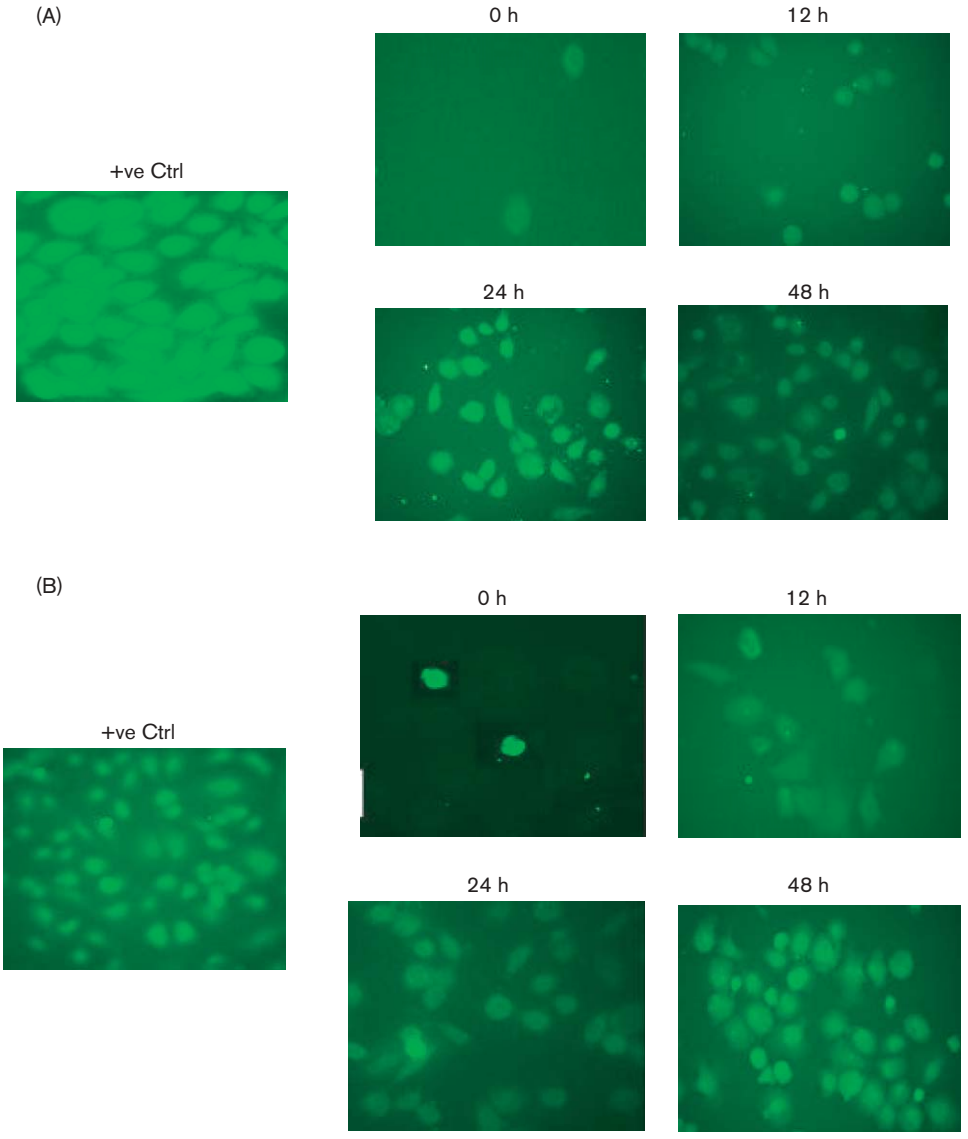

TQ treatment induces apoptosis in SP-1 (A) and I7 cells (B). Cells were grown on eight-well glass chambers (10^5 cells /ml) and treated with 30 μM TQ (SP-1), 60 μM TQ (I7) or methanol when 40–60% confluent. After 12, 24 or 48 h, cells were stained and mounted in Antifade as described in Materials and methods.

breaks due to apoptosis by terminal deoxynucleotidyl transferase. Our data revealed that, in comparison with control untreated cells, TQ-treated cells underwent an appreciable amount of apoptosis (Fig. 5). These findings confirmed that TQ-induced increases in the pre-G_1 fraction are due to apoptosis. The first apoptotic cells appeared 12 h after treatment with TQ. The proportion of apoptotic neoplastic keratinocytes increased in a time-dependent manner.

TQ modulation of key cell-cycle regulators

To further characterize the molecular basis of TQ-induced cellular effects, we investigated whether changes in the expression of key cell-cycle mediators accompany cell-cycle arrest induced by TQ. Since we observed G_1 phase arrest in TQ-treated SP-1 cells, we investigated the effects of TQ on the expression of p16 and p21 CDK inhibitors that are known to bind and antagonize cyclin/CDK complexes to halt G_1–S phase cell-cycle progression. In TQ-treated SP-1 cells, we also investigated the ability of this compound to modulate cyclin D and p53 protein levels. While cyclin D associates with CDK4 and CDK6 to form holoenzyme complexes that phosphorylate pRB and ensure G_1–S transition, p53 is a tumor suppressor protein that is known to play a major role in cell-cycle arrest and apoptosis. Although the expression of p53 and p21 proteins was not significantly altered upon treatment of SP-1 cells with TQ, we observed a dramatic increase in p16 protein levels (Fig. 6). Whereas basal levels of p16 proteins were undetectable in SP-1 cells, the levels sharply increased at 2 h post-TQ treatment, and the increase was sustained for up to 24 h and returned to basal undetectable levels at 48 h. In addition, the expression of cyclin D_1 proteins decreased 12 h post-TQ treatment (Fig. 6), while no major change in transcript levels was detected (data not shown), suggesting that the regulation is either at the translational or post-translational level. For I7 cells, we determined the effect of TQ on key cell-cycle modulators required for G_2/M transition such as cyclin B, p53 and p21. Interestingly, TQ-induced G_2/M arrest in I7 cells was associated with an increase in p53 protein at 4 h and a decrease in cyclin B protein at 8 h post-TQ treatment. There were no changes in the levels of p21 protein (Fig. 6).

TQ modulation of key apoptotic regulators

TQ treatment induced apoptosis in both cell lines was associated with the modulation of proapoptotic (Bax, Bak

Fig. 6

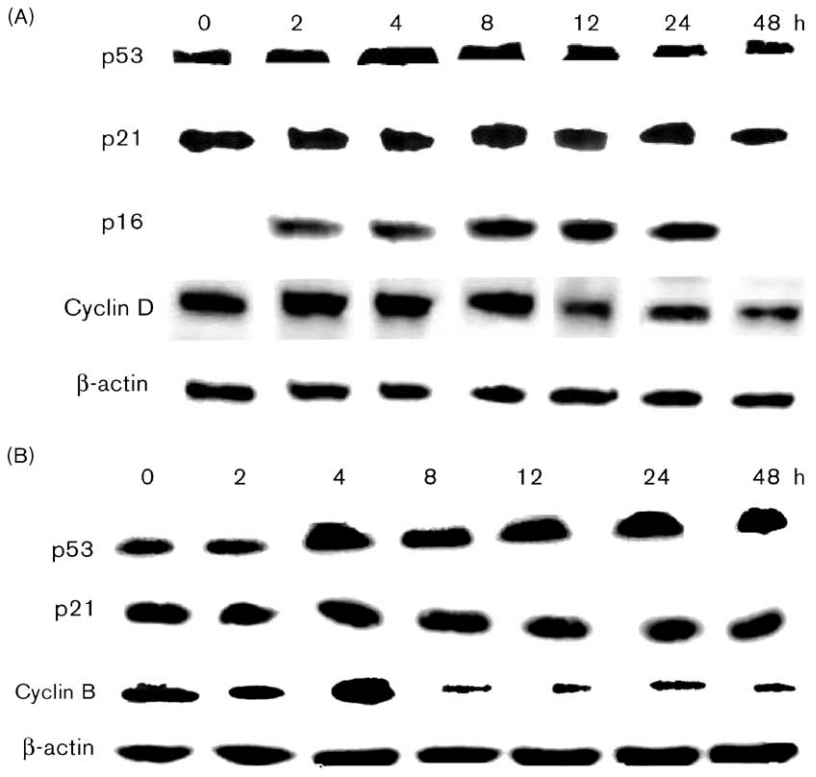

TQ treatment of SP-1 (A) or I7 (B) neoplastic keratinocytes results in differential expression of cell-cycle regulators. Cells were plated in 100-mm dishes at a density of 2×10^5 cells/ml and treated with less than 0.1% methanol, 30 μM TQ (SP-1) or 60 μM TQ (I7). Total SDS protein lysates were extracted from untreated control and TQ treated cells for 2, 4, 8, 12, 24 and 48 h. All blots were reprobed with β-actin to ensure equal protein loading.

and Bad) and antiapoptotic (Bcl-2, Bcl-$x_{L/S}$ and Bcl-w) protein (Fig. 7) and transcript (Fig. 8) levels. Bax, Bcl-2 and Bcl-$x_{L/S}$ are known to act on the mitochondria to regulate membrane permeability. The upregulation of Bax alters the ratio of the proapoptotic to antiapoptotic proteins in the cell leading to the release of cytochrome *c* to promote cell death. Interestingly, treatment of SP-1 cells with TQ resulted in a sharp increase in Bax protein levels as early as 2 h post-treatment (Fig. 7). However, no major change in Bax mRNA expression was detected in TQ-treated SP-1 cells (Fig. 8). The increase in Bax protein expression in I7 cells occurred at later times (24 h) following TQ treatment (Fig. 7). The levels of the antiapoptotic proteins Bcl-2 and Bcl-$x_{L/S}$ decreased in both cell lines (Fig. 8). In SP-1 cells, a sharp decrease in the transcript levels of antiapoptotic Bcl-$x_{L/S}$ and Bcl-w occurred at 12 h post-TQ treatment and the decrease was sustained for up to 48 h (Fig. 8).

Discussion

A wide range of naturally occurring agents have been identified as skin cancer chemopreventive agents [19,20]. An ideal agent is one that exerts cancer preventive effects with minimal or no toxicity and has a defined mechanism of action [19–21]. One such compound that we have previously investigated in our laboratories and found to inhibit the growth of colon cancer cells is TQ from black seed [22]. Despite the fact that TQ's antitumor activity has been well documented in various models, its mechanism of action is still unknown. Thus, we investigated TQ's effects in an *in vitro* skin model, i.e. the mouse papilloma SP-1 and spindle I7 cell lines, as well as normal counterpart cells, PMK, with the aim of

Fig. 7

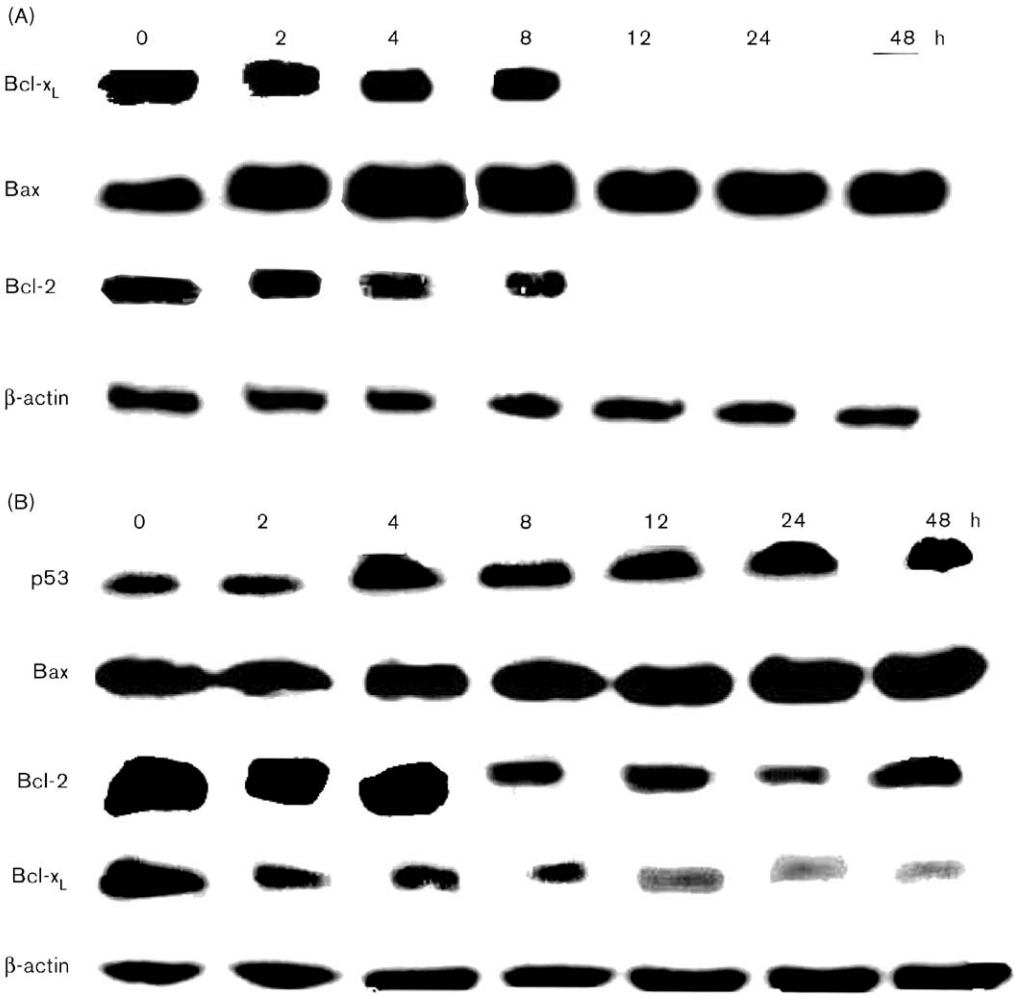

TQ treatment of SP-1 (A) or I7 (B) neoplastic keratinocytes results in differential expression of apoptosis markers. Cells were plated in 100-mm dishes at a density of 2×10^5 cells/ml and treated with less than 0.1% methanol or TQ. Total SDS protein lysates were extracted from untreated control and TQ-treated cells for 2, 4, 8, 12, 24 and 48 h. All blots were reprobed with β-actin to ensure equal protein loading.

Fig. 8

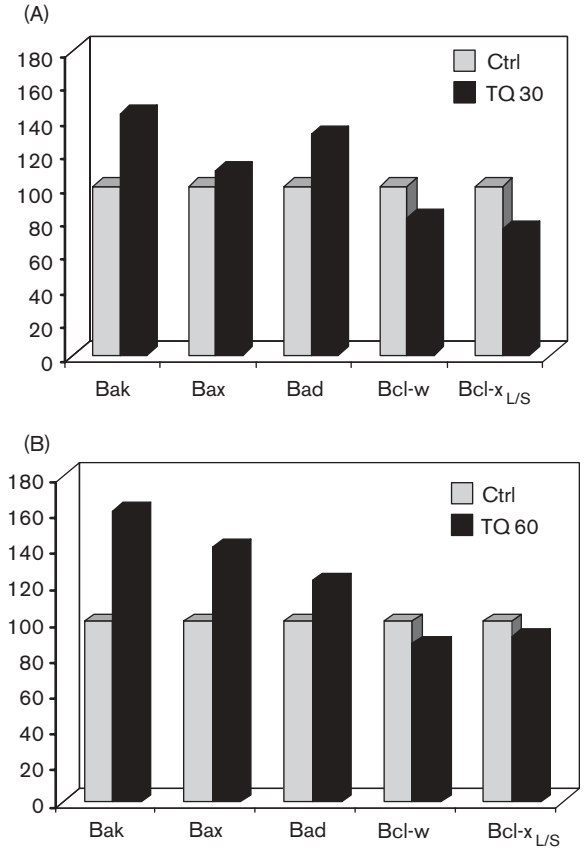

TQ treatment of SP-1 (A) or I7 (B) neoplastic keratinocytes modulates proapoptotic (Bax, Bak and Bad) and antiapoptotic (Bcl-w and Bcl-$x_{L/S}$) transcript levels. Cells were plated in 100-mm tissue culture dishes at a density of 2×10^5 cells/ml, and treated with 30 μM (SP-1) or 60 μM (I7) of TQ for 12 and 24 h, respectively. Total RNA was extracted from TQ-treated SP-1 and hybridized with specific probes against Bax, Bak, Bad, Bcl-$x_{L/S}$ and Bcl-w. The RNase protection assay was performed as described in Materials and methods. Net counts were obtained from each template (band) including L32. The values were normalized to L32 and results expressed as percentage of control cells for each group.

deciphering its antiproliferative mechanism of action at the cellular and molecular levels. Here we show that TQ inhibits the growth of neoplastic keratinocytes, induces cell-cycle arrest and apoptosis at non-cytotoxic concentrations.

SP-1 cells were more sensitive to the growth inhibitory effects of TQ than I7 cells. Growth inhibition in SP-1 cells was evident at half the concentrations of TQ and at shorter drug incubation times compared to I7 cells. This suggests that TQ treatment may be more effective when used at early stages of skin tumorigenesis. At late stages of skin carcinogenesis, cells may acquire mutations that lead to their greater resistance to TQ treatment. This is in accordance with other studies that have investigated natural compound effects and shown that cancer cells at advanced carcinogenic stages exhibit greater resistance to treatment [23,24].

The differential sensitivity of SP-1 and I7 cells to the growth inhibitory effects of TQ prompted us to investigate whether this is associated with differences on components of signaling pathways. Our flow cytometry results revealed that TQ treatment induces arrest at different phases of the cell cycle in the two cell lines. While short incubation times of TQ induced G_1 arrest in SP-1 cells, we observed G_2/M arrest in I7 cells. At longer incubation times and at higher doses, TQ induced apoptosis in the two cell lines. Thus, it is likely that TQ induces apoptosis in SP-1 cells by causing G_1 arrest and in I7 cells by causing G_2/M arrest. These effects correlated well with TQ's ability to differentially modulate the expression of components of signaling pathways involved in cell-cycle arrest and apoptosis. While TQ treatment tremendously induced p16 protein expression and inhibited cyclin D_1 expression in SP-1 cells, it increased p53 protein expression and inhibited cyclin B_1 protein levels in I7 cells.

The ability of TQ to remarkably increase p16 levels in SP-1 cells is very promising since the latter is a CDKI which is known to bind to CDK4/6 preventing its association with cyclin D, a requirement for G_1–S phase transition [25]. In addition, there is compelling evidence that the loss of p16 function occurs frequently in human cancers [25]. Thus, if TQ is capable of restoring p16 function in SP-1 papilloma cells, it is likely that it will play a role in the treatment of skin cancers at early stages of tumorigenesis. This is in agreement with others' findings showing that modulation of p16 expression increases the sensitivity of tumors to chemotherapeutic drugs [26]. The inhibition of cyclin D expression by TQ is also interesting since many anticancer drugs act by modulating this protein [27].

In I7 cells, TQ modulated the level of cyclin B_1 and p53 proteins, both of which are key regulators in the G_2 phase of the cell cycle. The tumor suppressor protein p53 is a critical component of the cellular mechanisms that respond to genotoxic stress to maintain the genomic integrity of the cell [9,28]. Recent studies have shown that the activation of p53 protein (post-translational modification) is necessary to induce G_2 arrest following DNA damage, since tumor cells lacking this protein enter into mitosis with accelerated kinetics [9,29,30]. The mechanism of p53-dependent G_2 arrest involves an initial inhibition of cyclin B_1/CDK1 activity by p21 protein, and the subsequent reduction of cyclin B_1 and CDK1 protein levels [30,31]. The reduced expression of cyclin B_1/CDK1 is mediated in part by p53-dependent repression of the cyclin B_1 and CDK1 promoters [30,32]. Many anticancer drugs currently used in the clinic exert their effects on p53 and cyclin B levels [33–37].

Whereas necrosis is a passive process of cellular metabolic collapse followed by cellular disintegration, apoptosis involves an active, energy-dependent mechanism in which cells participate in their own destruction [37]. Apoptosis is linked to the transcriptional activation of the proapoptotic Bax protein, and repression of the anti-apoptotic Bcl-2 and Bcl-x_L proteins, the generation of reactive oxygen species, and many other mechanisms [38,39]. Interestingly, the ability of TQ to induce apoptosis in SP-1 and I7 cells was associated with an increase in Bax protein expression and a drastic decrease in Bcl-$x_{L/S}$ and Bcl-w protein and transcript levels. Antiapoptotic Bcl-2 family members inhibit cell death by blocking cytochrome *c* release from the mitochondria, thereby preventing activation of the apoptosome pathway [40,41]. In contrast, Bax induces both cytochrome *c* release and caspase activation *in vitro* [42] and *in vivo* [43]. Overexpression of Bcl-2 could provide a survival advantage for cancer cells and has been associated with increased frequency of lymphoma development in a mouse model [44]. The increase in the Bcl-x_L expression level is very prominent in human ovarian carcinoma cells, and this contributes to the resistance of these cells to paclitaxel and cisplatin, drugs that are clinically used to treat ovarian cancers [45]. Loss of the proapoptotic Bax protein function might play a role in the pathogenesis of many types of cancer [46]. It is worth mentioning that TQ-induced upregulation of Bax protein occurred at earlier times and to a greater extent in SP-1 cells than in I7 cells. The increase in Bax expression occurred at 2 h post-TQ treatment in SP-1 cells and at 24 h in I7 cells, providing further support to the hypothesis that TQ treatment is more likely to exert its therapeutic and apoptotic effects at earlier stages of tumorigenesis.

The results presented in this study suggest a working model of TQ-induced cell-cycle arrest and apoptosis in SP-1 and I7 cells. This model reflects a balance between the ability of TQ to induce cell-cycle arrest, by modulation of p16 and cyclin D_1 in SP-1 cells and p53 and cyclin B_1 in I7 cells, and its ability to trigger apoptosis by modulation of Bax, Bcl-2 and Bcl-x_L proteins. In summary, this study identifies TQ as a potent inducer of cell-cycle arrest and apoptosis. The cytostatic and proapoptotic effects of TQ on skin cancer cells, in the absence of toxicity to primary keratinocytes, points to the potential use of this compound in the prevention and/or treatment of cancer. Further studies will focus on testing the effects of TQ treatment on other cell-cycle and apoptogenic regulators in an attempt to further dissect its mechanism of action.

Acknowledgments

We thank members of the Central Research Science Laboratory for their help in using the flow cytometer and fluorescence microscope. We thank Ms Ghada Abou-Lteif for help with the RNase protection assay.

References

1 Housman TS, Williford PM, Feldman SR, Teuschler HV, Fleischer AB Jr, Goldman ND, *et al.* Nonmelanoma skin cancer: an episode of care management approach. *Dermatol Surg* 2003; **29**:700–711.
2 Stratton SP, Dorr RT, Alberts DS. The state-of-the-art in chemoprevention of skin cancer. *Eur J Cancer* 2000; **36**:1292–1297.
3 Gali-Muhtasib HU, Schneider-Stock R. The medicinal potential of black seed (*Nigella sativa*) and its components. In: Khan MT (editor): *New Trends in Research Strategies on Lead Molecules from Natural Products*. Amsterdam: Elsevier; 2004: in press.
4 Salomi NJ, Satish C, Nair SC, Panikkar KR. Inhibitory effects of *Nigella sativa* and Saffron (*Crocus sativus*) on chemical carcinogenesis in mice. *Nutr Cancer* 1991; **16**:67–72.
5 Salomi NJ, Nair SC, Jayawardhanan KK, Varghese CD, Panikkar KR. Antitumour principles from *Nigella sativa* seeds. *Cancer Lett* 1992; **63**: 41–46.
6 Worthen DR, Ghosheh OA, Crooks PA. The *in vitro* anti-tumor activity of some crude and purified components of blackseed, *Nigella sativa* L. *Anticancer Res* 1998; **18**:1527–1532.
7 Nagi MN, Mansour MA. Protective effect of thymoquinone against doxorubicin-induced cardiotoxicity in rats: a possible mechanism of protection. *Pharmacol Res* 2000; **41**:283–289.
8 Soussi T. The p53 tumour suppressor gene: a model for molecular epidemiology of human cancer. *Mol Med Today* 1996; **2**:32–37.
9 Levine AJ. p53, the cellular gatekeeper for growth and division. *Cell* 1997; **88**:323–331.
10 Kagawa S, Fujiwara T, Hizuta A, Yasuda T, Zhang WW, Roth JA, *et al.* p53 expression overcomes $p21^{WAF1WAF1}$/CIP1-mediated G_1 arrest and induces apoptosis in human cancer cells. *Oncogene* 1997; **15**: 1903–1909.
11 Kokontis JM, Wagner AJ, O'Leary M, Liao S, Hay N. A transcriptional activation function of p53 is dispensable for and inhibitory of its apoptotic function. *Oncogene* 2001; **20**:659–668.
12 Han Z, Wei W, Dunaway S, Darnowski JW, Calabresi P, Sedivy J, *et al.* Role of $p21^{WAF1}$ in apoptosis and senescence of human colon cancer cells treated with camptothecin. *J Biol Chem* 2002; **277**: 17154–17160.
13 Niculescu III AB, Chen X, Smeets M, Hengst L, Prives C, Reed SI. Effects of p21(Cip1/Waf1) at both the G_1/S and the G_2/M cell cycle transitions: pRb is a critical determinant in blocking DNA replication and in preventing endoreduplication. *Mol Cell Biol* 1998; **18**:629–643.
14 Medema RH, Klompmaker R, Smits VA, Rijksen G. $p21^{waf1}$ can block cells at two points in the cell cycle, but does not interfere with processive DNA-replication or stress-activated kinases. *Oncogene* 1998; **16**: 431–441.
15 Shen Y, White E. p53-dependent apoptosis pathways. *Adv Cancer Res* 2001; **82**:55–84.
16 Moravec R. Total cell quantitation using the CytoTox 96™ Non-Radioactive Cytotoxicity Assay. *Promega Notes* 1994; **45**:11–12.
17 Strickland JE, Greenhalgh DA, Koceva-Chyla A, Hennings H, Restrepo C, Balaschak M, *et al.* Development of murine epidermal cell lines which contain an activated ras^{Ha} oncogene and form papillomas in skin grafts on athymic nude mouse hosts. *Cancer Res* 1988; **48**:165–169.
18 Greenhalgh DA, Welty DJ, Player A, Yuspa SH. Two oncogenes, v-*fos* and v-*ras,* cooperate to convert normal keratinocytes to squamous cell carcinoma. *Proc Natl Acad Sci USA* 1990; **87**:643–647.
19 Koyama J, Morita I, Tagahara K, Nobukuni Y, Mukainaka T, Kuchide M, *et al.* Chemopreventive effects of emodin and cassiamin B in mouse skin carcinogenesis. *Cancer Lett* 2002; **182**:135–139.
20 Gupta S, Mukhtar H. Chemoprevention of skin cancer through natural agents. *Skin Pharmacol Appl Skin Physiol* 2001; **14**:373–385.
21 Kapadia GJ, Azuine MA, Tokuda H, Takasaki M, Mukainaka T, Konoshima T, *et al.* Chemopreventive effect of resveratrol, sesamol, sesame oil and sunflower oil in the Epstein–Barr virus early antigen activation assay and the mouse skin two-stage carcinogenesis. *Pharmacol Res* 2002; **45**:499–505.
22 Gali-Muhtasib HU, Diab-Assaf M, Boltze C, Al-Hmaira J, Roessner A, Schneider-Stock R. Thymoquinone induces apoptosis in human colorectal cancer HCT-116 cells through a p53-dependent mechanism. *Mol Pharmacol* 2004; in press.
23 Higgins CF, Callaghan R, Linton KJ, Rosenberg MF, Ford RC. Structure of the multidrug resistance P-glycoprotein. *Semin Cancer Biol* 1997; **8**:135–142.

24 Riordan JR, Deuchars K, Kartner N, Alon N, Trent J, Ling V. Amplification of P-glycoprotein genes in multidrug-resistant mammalian cell lines. *Nature* 1985; **316**:817–819.
25 Sherr CJ. The Pezcoller lecture: cancer cell cycles revisited. *Cancer Res* 2000; **60**:3689–3695.
26 Hochhauser D. Modulation of chemosensitivity through altered expression of cell cycle regulatory genes in cancer. *Anticancer Drugs* 1997; **8**:903–910.
27 Chang HC, Weng CF, Yen MH, Chuang LY, Hung WC. Modulation of cell cycle regulatory protein expression and suppression of tumor growth by mimosine in nude mice. *Int J Oncol* 2000; **17**:659–665.
28 Somasundaram K, El-Deiry WS. Tumor suppressor p53: regulation and function. *Front Biosci* 2000; **5**:424–437.
29 Bunz F, Dutriaux A, Lengauer C, Waldman T, Zhou S, Brown JP, *et al.* Requirement for p53 and p21 to sustain G_2 arrest after DNA damage. *Science* 1998; **282**:1497–1501.
30 Flatt PM, Pietenpol JA. Mechanisms of cell-cycle checkpoints: at the crossroads of carcinogenesis and drug discovery. *Drug Metab Rev* 2000; **32**:283–305.
31 Innocente SA, Abrahamson JL, Cogswell JP, Lee JM. p53 regulates a G_2 checkpoint through cyclin B_1. *Proc Natl Acad Sci USA* 1999; **96**:2147–2152.
32 Taylor WR, DePrimo SE, Agarwal A, Agarwal ML, Schonthal AH, Katula KS, *et al.* Mechanisms of G_2 arrest in response to overexpression of p53. *Mol Biol Cell* 1999; **10**:3607–3622.
33 Augustin E, Wheatley DN, Lamb J, Konopa J. Imidazoacridinones arrest cell-cycle progression in the G_2 phase of L1210 cells. *Cancer Chemother Pharmacol* 1996; **38**:39–44.
34 Lamb J, Wheatley DN. Cell killing by the novel imidazoacridinone antineoplastic agent, C-1311, is inhibited at high concentrations coincident with dose differentiated cell cycle perturbation. *Br J Cancer* 1996; **74**:1359–1368.
35 Calabrese CR, Bibby MC, Double JA, Loadman PM. Pharmacokinetics and tissue distribution of the imidazoacridinone C1311 in tumour-bearing mice. *Cancer Chemother Pharmacol* 1998; **42**:379–385.
36 Zaffaroni N, De MarcoC, Villa R, Riboldi S, Daidone MG, Double JA. Cell growth inhibition, G_2M cell-cycle arrest and apoptosis induced by the imidazoacridinone C1311 in human tumour cell lines. *Eur J Cancer* 2001; **37**:1953–1962.
37 Evan G, Littlewood T. A matter of life and cell death. *Science* 1998; **281**:1317–1322.
38 Miyashita T, Reed JC. Tumor suppressor p53 is a direct transcriptional activator of the human *bax* gene. *Cell* 1995; **80**:293–299.
39 Yin C, Knudson CM, Korsmeyer SJ, Van Dyke T. Bax suppresses tumorigenesis and stimulates apoptosis *in vivo*. *Nature* 1997; **385**: 637–640.
40 Kluck RM, Bossy-Wetzel E, Green DR, Newmeyer DD. The release of cytochrome *c* from mitochondria: a primary site for Bcl-2 regulation of apoptosis. *Science* 1997; **275**:1132–1136.
41 Yang J, Liu X, Bhalla K, Kim CN, Ibrado AM, Cai J, *et al.* Prevention of apoptosis by Bcl-2: release of cytochrome c from mitochondria blocked. *Science* 1997; **275**:1129–1132.
42 Jurgensmeier JM, Xie Z, Deveraux Q, Ellerby L, Bredesen D, Reed JC. Bax directly induces release of cytochrome *c* from isolated mitochondria. *Proc Natl Acad Sci USA* 1998; **95**:4997–5002.
43 Stepczynska A, Lauber K, Engels IH, Janssen O, Kabelitz D, Wesselborg S, *et al.* Staurosporine and conventional anticancer drugs induce overlapping, yet distinct pathways of apoptosis and caspase activation. *Oncogene* 2001; **20**:1193–1202.
44 McDonnell TJ. Bcl-2–immunoglobulin transgenic mice demonstrate extended B cell survival and follicular lymphoproliferation. *Cell* 1989; **57**:79–88.
45 Rogers PM, Beale PJ, Al-Moundhri M, Boxall F, Patterson L, Valenti M, *et al.* Overexpression of Bcl_{XL} in a human ovarian carcinoma cell line: paradoxic effects on chemosensitivity *in vitro* versus *in vivo*. *Int J Cancer* 2002; **97**:858–863.
46 Rampino N, Yamamoto H, Ionov Y, Li Y, Sawai H, Reed JC, *et al.* Somatic frameshift mutations in the BAX gene in colon cancers of the microsatellite mutator phenotype. *Science* 1997; **275**:967–969.